IEEE Access
Multidisciplinary | Rapid Review | Open Access Journal

Received January 23, 2018, accepted February 19, 2018, date of publication February 27, 2018, date of current version March 13, 2018.

Digital Object Identifier 10.1109/ACCESS.2018.2809448

Simultaneous Determination of Modulation Types and Signal-to-Noise Ratios Using Feature-Based Approach

TARIK ADNAN ALMOHAMAD, (Student Member, IEEE), MOHD FADZLI MOHD SALLEH, (Member, IEEE), MOHD NAZRI MAHMUD, AND ADNAN HAIDER YUSEF SA'D, (Student Member, IEEE)

School of Electrical and Electronic Engineering, Universiti Sains Malaysia, Seri Ampangan, 14300 Nibong Tebal, Pulau Pinang, Malaysia

Corresponding authors: Tarik Adnan Almohamad (tam_jami@hotmail.com) and Mohd Fadzli Mohd Salleh (fadzlisalleh@usm.my)

This work was supported in part by the Universiti Sains Malaysia under Research University Individual under Grant 1001/PELECT/814203 and in part by USM fellowship.

ABSTRACT This paper presents a low-complexity technique for simultaneous determination of modulation types and signal-to-noise ratios (SNRs) in wireless communication systems. The proposed approach exploits the extracted features of patterns observed in signals' asynchronous amplitudes histograms, for the simultaneous determination of these quantities using support vector machine. Features extraction has been performed by a well-known technique called principal component analysis which is used to extract the most significant features before being supplied to the artificial intelligent system. Simulations for three commonly-used modulation types have been conducted under real-world channel conditions. The results conclude that the presented approach can accurately identify the modulation types with 99.83% accuracy despite the existence of real-world channel impairments. Furthermore, the algorithm is capable of SNRs estimation over a broad range of 0–30 dB with average estimation error of 0.79 dB. The proposed paper exploits the simplicity of generating asynchronous amplitudes histograms to enable cost-effective and reduced-complexity implementation in cognitive wireless systems.

INDEX TERMS Simultaneous determination, modulation recognition, SNR estimation, support vector machine, feature-based approach, cognitive wireless systems.

I. INTRODUCTION

The last few decades have witnessed many techniques for the estimation of signals' parameters such as modulation type, signal-to-noise ratio (SNR), bit-rate, transmitted signal power etc., in wireless communications [1]–[5] . The transmitters in future wireless networks are anticipated to vary these parameters according to the given channel conditions. This, in turn, will necessitate the receivers employed in these networks to be effectively prepared of autonomous estimation of various signal parameters. Most of the existing solutions focus on determining a single parameter for e.g., modulation format [6]–[15] or signal-to-noise ratio (SNR) [16]–[19] rather than on estimating multiple parameters jointly. More recently, a few techniques for simultaneous determination of multiple signal parameters have been reported in the literature such as the asynchronous delay-tap plots (ADTPs)-based technique proposed in [20] and [21]. One drawback of this technique is that it requires two sampling devices. Furthermore, the tap-delay between the two samplers needs to be adjusted according to the data rates of the transmitted signals which in turn increases the implementation complexity [22]. The contributions of this paper lie in two folds; the first one is to propose a technique that can jointly estimate modulation types and SNRs of received signals in multipath fading channels using machine learning algorithm. The second is to reduce the implementation complexity by exploiting the most important features of asynchronous amplitude histograms (AAHs) the generation of which requires only a single low-speed asynchronous sampling device. In the presented algorithm, we employ a supervised learning method namely support vector machine (SVM) in conjunction with AAHs. SVMs have proven their superior recognition capabilities as compared to other conventional methods such as artificial neural networks in several pattern recognition applications [23], [24]. In this work, we use extracted features of AAHs using PCA for the training of SVM-based classifier

and regressor. To analyze the capability of the proposed approach, numerical simulations have been performed for three modulation formats namely 2ASK, QPSK and 16QAM with bit-rates of 250 Mbps, 500 Mbps and 1 Gbps, respectively, and having SNRs vary from 0 to 30 dB. The results validate successful determinations of modulation types and SNRs with high estimation accuracies.

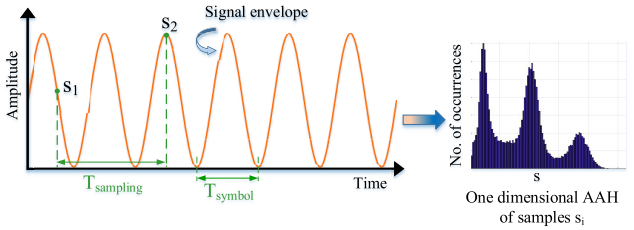

FIGURE 1. Principle of AAH by using asynchronous signal envelope sampling. T_{symbol} & $T_{sampling}$ refer to symbol period and sampling period respectively.

II. ASYNCHRONOUS AMPLITUDES HISTOGRAMS

Asynchronous amplitude histogram (AAH) is one of asynchronous sampling-based techniques that offers cost-effectiveness, low-complexity and flexibility in implementation. Fig. 1 illustrates how AAH is produced. The steps of an AAH generation can be described as follows: first, the received signal envelope is arbitrarily sampled at a sampling rate, that is much lower than but unrelated to its symbol rate. Then, the samples are ordered according to the magnitudes of their voltage amplitudes $S = \{s_n | n = 1, \ldots, N$, where N is the number of samples. After that, the total range of voltage amplitudes $[V_{min} V_{max}]$ is equally split into M histogram bins as follows:

$$b = [[V_{min}, V_1], (V_1, V_2], \ldots, (V_{m-1}, V_m], (V_m, V_{m+1}], \ldots, \ldots, (V_{M-1}, V_M]] \quad (1)$$

where b describes the voltage amplitude of samples in each bin, V_{min} and V_{max} represent the minimum and maximum voltage amplitude of samples $S \in [V_{min}, V_{max}]$ respectively and V_m is expressed as:

$$V_m = V_{min} + m(V_{max} - V_{min})/M \quad (2)$$

The sample values S are then mapped onto the bins $\mathbf{s}^{(m)}$ (that is, $\mathbf{s}^{(m)}$ is a group of samples that have values within the range $(V_{m-1}, V_m]$). The number of occurrences of the amplitude samples that lie within each of the bins' range are calculated using the formula:

$$\mathcal{N} = [n\left(\boldsymbol{s}^{(1)}\right), n\left(\boldsymbol{s}^{(2)}\right), \ldots, n\left(\boldsymbol{s}^{(M)}\right)] \quad (3)$$

where $\mathcal{N}$ represents the number of occurrences vector and $n(.)$ denotes a number of samples that has been mapped onto $\boldsymbol{s}^{(m)}$. Finally plotting the number of occurrences as a function of bin number, the amplitude histogram is then generated [25].

AAHs offer cost-effectiveness and low-complexity due to the utilization of a single sampler which operates at low sampling speed i.e., the sampling period $T_{sampling}$ is much longer than the symbol period T_{symbol}. Furthermore, the sampling rate is totally not associated with the symbol rate. This points out that the synchronous timing information is inessential.

AAHs exhibit unique statistical attributes which can be exploited to obtain critical knowledge about different signals' parameters such as modulation type and SNR. The unique signatures reflected by AAHs enable the recognition of modulation types of different received signals. In addition, the shapes of AAHs also change when SNR values are varied, and remain distinguishable from each other. This means that AAH can be exploited to simultaneously recognize the modulation type and estimate the SNR value. The simultaneous operation signifies the improvement over most of the existing work that requires two separate operations to determine the aforementioned parameters [6]–[19]. Having a pre-knowledge of the modulation type and SNR, is vital to receivers in future wireless communication systems. This crucial information will enable many functions at the receivers such as supporting the signal's demodulators and anticipating the potential changes at the transmitters such as dynamic power allocation, adaptive schemes of modulations, etc.

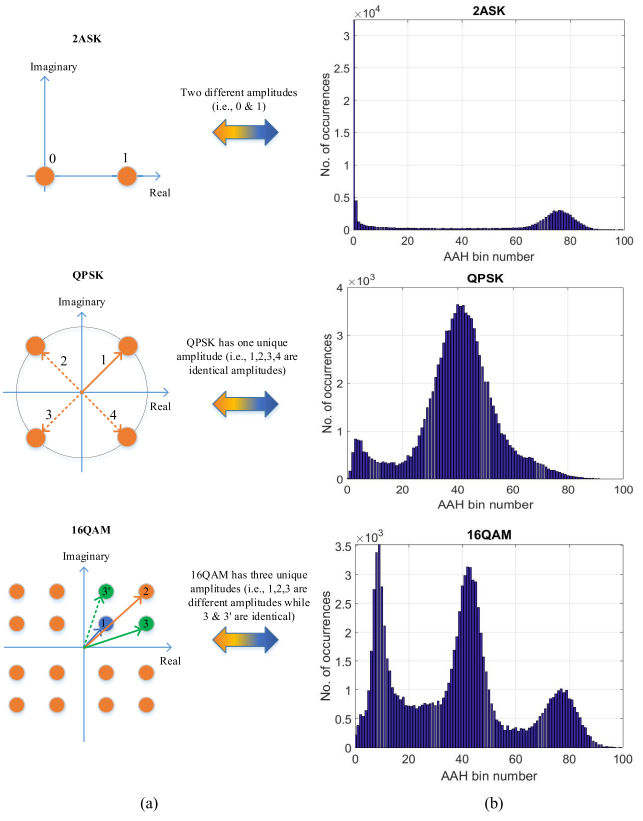

FIGURE 2. The conceptual background behind the diversity of AAHs-based signals. (a) Complex Plane (b). Asynchronous Amplitudes Histograms.

Fig. 2 illustrates the idea behind the differences in histogram shape among signals with various modulations

considered in the proposed work i.e., 2ASK, QPSK and 16QAM. In the left column (a) of the figure, the constellation diagram for every modulation is shown. 2ASK signal has two different constellation points (i.e. amplitude levels 0 & 1), hence two distinct peaks in the corresponding AAH will appear, that is, first peak always represents "0" amplitude and the other one denotes "1" amplitude. In QPSK diagram, the four amplitudes labeled 1,2,3,4 are equally distributed in the real-imaginary coordinates which results in a QPSK histogram with one common amplitude; therefore its corresponding AAH will consist of a single peak as shown in the right column (b) of the Fig. 2. The number of AAH-peaks in 16QAM signal will be higher than the aforementioned two signals. As shown in the complex plane column (a), the 16QAM constellation diagram has three unique amplitudes (illustrated in different colors i.e., blue: (1), orange: (2) and green: (3 and 3`). That signifies the existence of three peaks in 16QAM histogram shape.

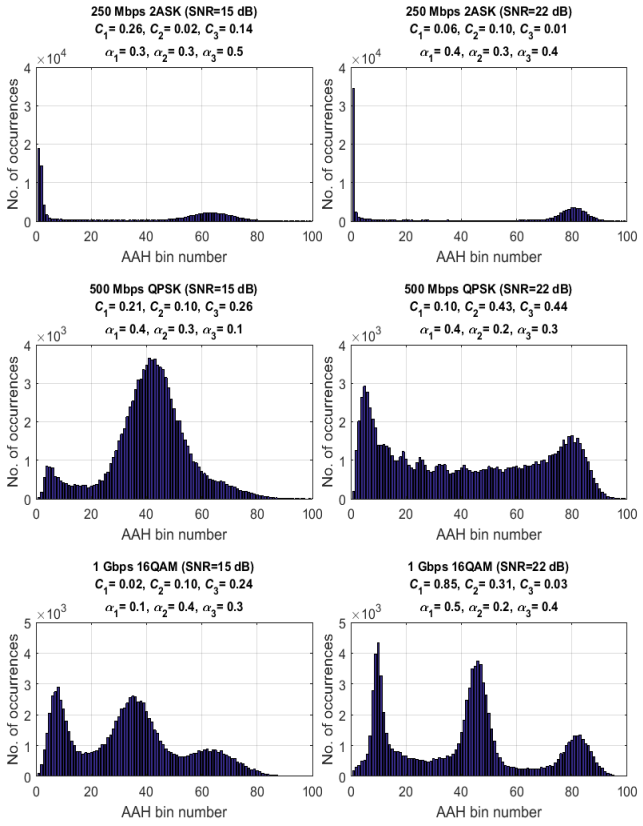

FIGURE 3. AAHs for different modulation formats, SNRs, channel coefficients and path delays.

Fig. 3 illustrates AAHs for three modulation types considered in this work for two different SNRs. It is obvious from the figure that the histograms corresponding to different modulation formats, SNRs, path delays and fading-channel coefficients are distinguishable from each other.

With the aim of lowering the processing complexity of the proposed algorithm, the most useful features of the signals' histograms are extracted using the PCA technique. The extracted features are then used to train the SVMs for the simultaneous determination of the modulation type and SNR of the detected signal.

III. ALGORITHM MECHANISM

The unique features of these AAHs can thus be exploited for simultaneous determination of modulation formats and SNRs by utilizing pattern recognition methods such as SVM-based systems. In this work, we employ two different types of SVMs. The first one, called support vector classifier (SVC), is used for the determination of modulation type while the second, namely support vector regressor (SVR), is utilized for SNR estimation. Fig. 4 shows SVM-based classifier and regressor with AAH bin-count vectors x as inputs of both SVMs and the determined modulation formats and SNRs as outputs.

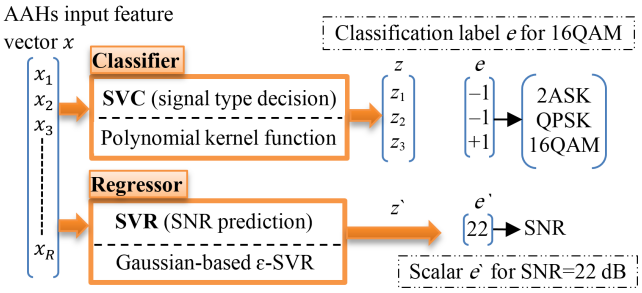

FIGURE 4. SVMs with AAH bin-count vectors x as inputs and determined modulation formats and SNRs as outputs. The output vector z contains a '+1' element and '−1s' elsewhere.

Each AAH is represented by bin-count vector x and its corresponding label e and scalar $e^{\backprime}$. Label vector e contains two '−1' elements and a single '+1' element whose position signifies the signal type, whereas scalar $e^{\backprime}$ indicates the value of SNR pertaining to that AAH. The outputs z and $z^{\backprime}$ are expected to match the corresponding label e and the actual value $e^{\backprime}$ respectively.

Both SVC and SVR are trained in a supervised manner by utilizing bin-count vectors x as inputs while label e and scalar $e^{\backprime}$ as targets illustrated in Fig. 4.

In this work, we use one-against-all approach which is a popular strategy in multi-class SVMs to construct three SVC models. Each SVC is trained to differentiate a modulation type ('+1') from the other two modulation types ('−1') using a cubic polynomial kernel. This kernel function maps the training samples into a higher dimensional space in order to construct an optimal hyperplane (the maximum margin between positive and negative classes) which separates samples of each class from the remaining classes. On the other hand, for the regression task, the algorithm implements an epsilon-SVR (ε-SVR). The aim is to obtain a function that deviates from the label $e^{\backprime}$ by no more than ε for every training sample. The performance of the trained-SVM models is evaluated by utilizing a testing data set which is a part from the entire data set. In the testing phase, vectors x from the testing data set are applied simultaneously at both SVMs'

inputs and corresponding outputs z and $z^{\backprime}$ are obtained. Due to the binary nature of SVM classifiers, the SVC output vector z will have a single '+1' element and '−1s' elsewhere. Hence, argmax$\{z\}$, or the position of '+1' returns the identified modulation type.

On the other hand, the scalar output $z^{\backprime}$ of SVR directly provides SNR estimate. Finally, a comparison is made between the estimated and actual modulation types and SNRs, and estimation accuracies are calculated. We performed 50 iterations for the simulation of SNR estimation and then calculated the mean SNR estimation error.

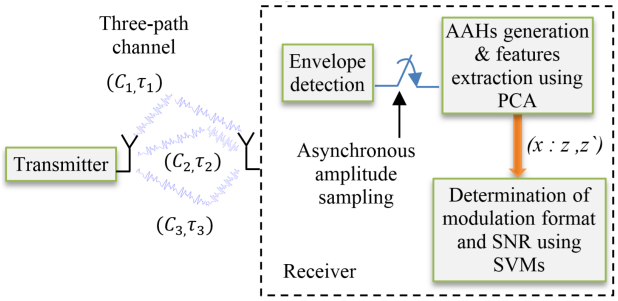

FIGURE 5. The system model used in simulations.

IV. SYSTEM MODEL

The system model utilized for evaluating the performance of the proposed technique is illustrated in Fig. 5. Our system model employs the parameters shown in Table 1.

TABLE 1. Values/ranges of parameters used in the simulations.

Parameter	Quantity
Modulation formats/bit-rates	250 Mbps 2ASK, 500 Mbps QPSK, 1 Gbps 16QAM
SNR	0–30 dB
Channel type	Multipath fading
Coefficients C_i and α_i	Uniformly distributed in the range of 0–1 and 0–0.5, respectively

Table 1 shows the values and ranges of various simulation parameters. The Gaussian filters are used for shaping the signal pulses before transmission over a three-path channel. To analyze the recognition ability of the proposed algorithm for diverse modulations, three types of modulation formats (2ASK, QPSK, 16QAM) are considered since they belong to various categories of amplitude and phase modulation schemes. The SNR values of the signals are incremented by 1dB in the interval of 0–30 dB. Each of three paths has a different coefficient C_i where its value is set in a uniformly random manner between 0 and 1. Also, each path has a random delay τ_i as shown in (4):

$$\tau_i = T_{\mathrm{LoS}} + \alpha_i T_{\mathrm{s}} \tag{4}$$

where T_{LoS} is the line-of-sight path's delay, α_i are uniformly-distributed random variables in the interval between 0 and 0.5,

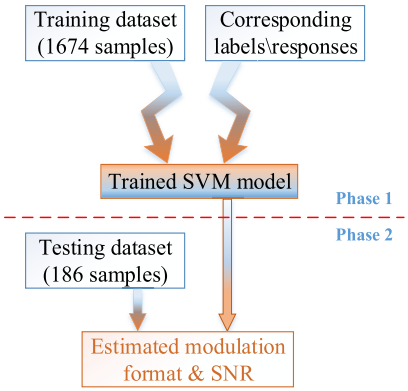

FIGURE 6. A flow diagram for supervised learning algorithm.

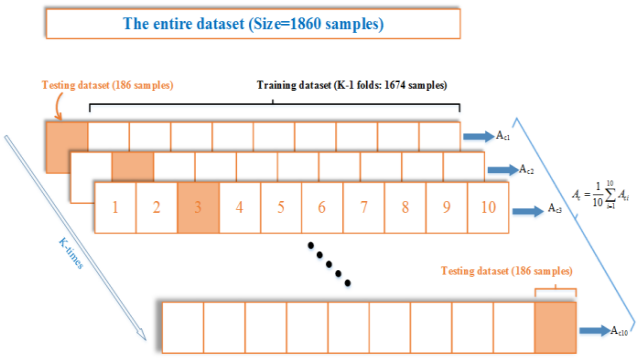

FIGURE 7. 10-fold cross-validation technique.

and T_{s} is the symbol period. At the receiver, non-coherent detection is performed to detect the envelope of the received signal. Next, asynchronous amplitude sampling is used to obtain the samples of signal's envelope. We acquired a total of 100,000 samples which are then employed for the synthesis of histograms with 100 bins.

A large data set consists of 1860 AAHs derived from 3 types of signals, 31 SNRs, and 20 arbitrary combinations of channel coefficients and path delays (i.e., $1860 = 3 \times 31 \times 20$). AAHs in the large data set are partitioned into training and testing data sets by K-fold cross-validation method.

The block diagram in Fig. 6 illustrates the execution process of supervised learning algorithm (i.e., SVM) as two phases. At the first phase, the training dataset with its associated labels are used to generate a trained SVM model. In the second phase, the performance of the trained SVM model is evaluated using a new testing dataset to estimate the required parameters (i.e., modulation type & SNR value).

In K-fold cross-validation technique, the entire data set is arbitrarily segregated into a number of equal-size K-subsets. A K-subset is utilized once for testing process while the remaining K-1 subsets are combined and utilized for training the SVM classifier and regressor in order to obtain the trained model. The cross-validation procedure is recurred K-times and a K-subset will uniquely act as a testing data set once

every iteration. Finally, the overall determination accuracy of the whole K-iterations is calculated. The determination accuracy is defined as:

$$A_{ci} = \frac{C_s}{E_s} \times 100\% \tag{5}$$

where C_s is the number of correctly classified samples and E_s is the size of entire testing data set.

In this paper, the data set is partitioned using two types of cross-validation methods (i.e., *5-fold cross-validation* and *10-fold cross-validation*) in order to investigate the size's effect of testing data set on the overall determination accuracy. Fig. 7 illustrates the scenario of 10-fold cross-validation.

As shown in Fig. 7, in each iteration, the entire AAHs in the large data set are partitioned into training and testing data sets by arbitrarily choosing 90% (i.e., 1674) and 10% (i.e., 186) of total AAHs, respectively. These new data groups are then used for the training and testing processes of SVM models. Each AAH in the two datasets is represented by a 100×1 vector x of bin-counts. In addition, for every AAH in the training data set, we generated a 3×1 label vector e (containing two '-1' elements and a single '$+1$' element whose position signifies the signal type corresponding to that AAH) and a scalar label $e^{\backslash}$ which indicates the value of SNR pertaining to that AAH.

V. FEATURES EXTRACTION USING PRINCIPAL COMPONENT ANALYSIS

With the aim of extracting the most useful and distinguished features of the signals' histograms and lowering the processing complexity of the proposed algorithm, a well-known technique called PCA is utilized in this work. PCA has become an attractive choice to a wide range of real-world applications in many disciplines such as feature extraction, learning algorithms and pattern recognition [26]–[28]. The purpose of PCA technique's implementation is to drastically decrease the dimensionality of the data space and transform it to a new subspace of descriptive features and maintaining the general data distribution. This new derived space comprises uncorrelated variables named principal components (PCs) which have highest variances and preserve most of the important statistics of the original data.

There are many techniques being deployed to extract the principal components such as eigenvalue decomposition (ED), the power algorithm, singular value decomposition (SVD). However, SVD has received a vital attention of many researchers recently and it has been exploited in many different research areas such as image processing and data analysis. In addition, SVD plays a vital role in subspace estimation, least squares techniques and finding eigenvectors. Therefore, we have chosen SVD in this proposed scheme.

In this work, we apply SVD-based PCA technique on the AAHs in both training and testing data sets to extract the most significant features. The SVD is utilized in order to extract the eigenvectors and eigenvalues required to construct the PCs.

The following steps summarize the implementation of PCA:

1- Consider a matrix Q $(n \times p)$ where n represents the AAHs and p signifies the number of variables. In matrix Q, each vector q_{i} represents an AAH which corresponds to different signal type with various SNRs. The definition of the mean AAH vector β of the matrix Q is given by:

$$\beta = \frac{1}{n}\sum_{i=1}^{n} q_i \tag{6}$$

2- Obtain the zero-mean matrix Y by subtracting β from every column of matrix Q, i.e., $Y = [y_1, y_2, \ldots, y_n]$, where $y_i = q_i - \beta$. We find the covariance matrix C of Y as follows:

$$C = \frac{1}{n} YY^T \tag{7}$$

where C is symmetric matrix i.e. diagonalizable.

3- Perform SVD algorithm on matrix Y, we get the decomposition as shown in (8):

$$Y = USV^T \tag{8}$$

where S is a matrix that includes the singular values s_i. By substituting (8) in (7), we obtain:

$$C = USV^T (USV^T)^T \frac{1}{n} = USV^T \left(VSU^T\right) \frac{1}{n} \tag{9}$$

Since $V^T.V = I$ (i.e., orthogonal matrix), therefore:

$$C = U\frac{S^2}{n}U^T \tag{10}$$

The relation between the singular values s_i and the eigenvalues λ_i of the covariance matrix is given by:

$$\lambda_i = \frac{S^2}{n} \tag{11}$$

However, the eigenvalues can be calculated through the following equation:

$$C\gamma_i = \lambda_i \gamma_i, \quad i = 1, 2, \ldots, p \tag{12}$$

where p is the number of eigenvectors (PCs) equals to 100.

The PCs i.e. eigenvectors are sorted from the highest to the lowest based on their corresponding eigenvalues. A selected number of eigenvectors R (where $R < p$) corresponding to their largest eigenvalues, is chosen for the next training and testing stages while ignoring the remaining eigenvectors. The following criterion will determine the selection of R-value:

$$\nabla = \sum_{i=1}^{R} \lambda_i \Big/ \sum_{i=1}^{p} \lambda_i > M_c \tag{13}$$

where the typical determination of M_c value is made to be larger than 0.9 [28], [29].

The selected PCs are the eigenvectors of the covariance matrix C, i.e., the columns of matrix U. Finally, these PCs

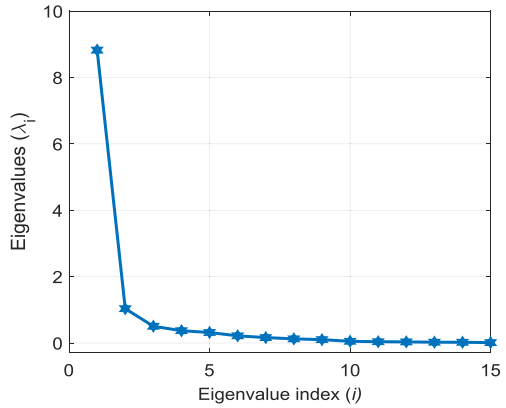

FIGURE 8. Eigenvalues λ_i for some selected PCs are in descending order.

span a new R-dimensional subspace of the original space of data matrix Q. An approximation of a weighted-sum of the selected PCs can be represented as a vector y that pertains to a given AAH (train\test datasets) as shown below:

$$y \approx \sum_{i=1}^{R} x_r \gamma_r \Longrightarrow x_r = \gamma_r^T y, \quad \text{for } r = 1, 2, \ldots, R \qquad (14)$$

Therefore, the feature vector x of a given AAH will include the weights x_r i.e., $x = [x_1, x_2, \ldots, x_R]^T$. The relation between the eigenvalues of chosen significant PCs and their indices is illustrated in Fig. 8. It can be seen from Fig. 8 that these eigenvalues λ_i are graded from the largest to the lowest and dramatically approaching zero.

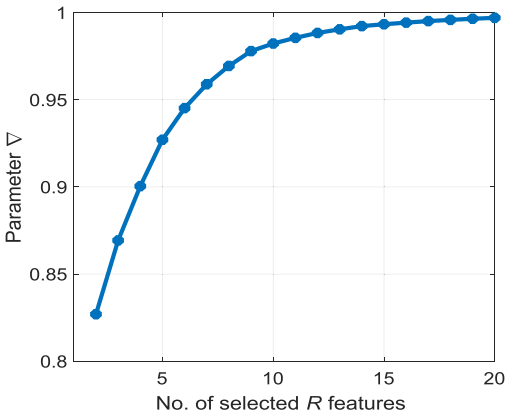

FIGURE 9. The relation between parameter ∇ and the selected R principal components (features).

Fig. 9 presents the relation between the selected R features and parameter ∇ which varies based on the quantity of the PCs chosen R.

It is illustrated in the figure that when six features are chosen ($R = 6$), the value of parameter ∇ is greater than 0.94. Hence, it proves the efficiency of exploiting a few PCs rather than utilizing the entire features. This will lead towards less computational complexity and faster processing for the implementation of the proposed recognition technique.

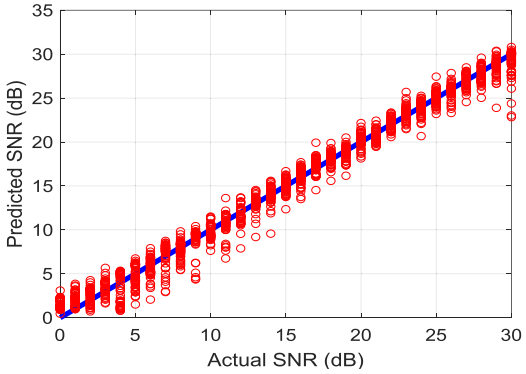

FIGURE 10. Actual versus estimated SNRs for the proposed estimation technique.

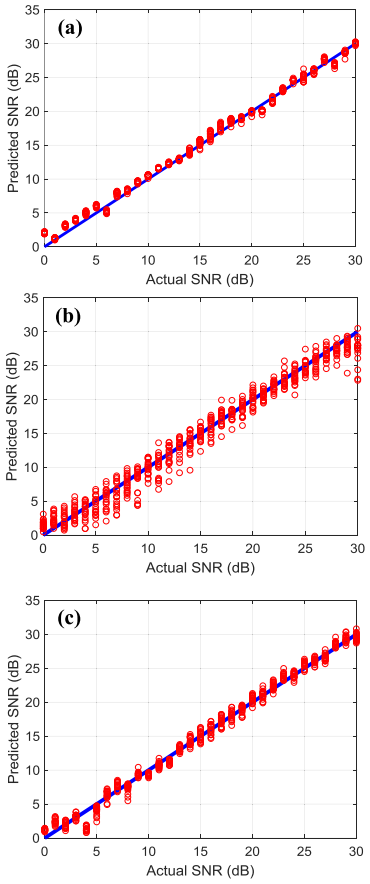

FIGURE 11. Actual versus estimated SNRs for (a) 2ASK signal, (b) QPSK signal, (c) 16QAM signal using the proposed scheme.

VI. SIMULATION RESULTS

Fig. 10 illustrates the results of SNR estimations for the three signals. As proven in the figure, the estimated SNR values are quite close to the actual values. The mean SNR estimation error calculated over the SNR range of 0–30 dB is 0.79 dB for 186 testing cases.

Fig. 11 illustrates the estimated against the actual SNR values for every signal i.e., (a) 2ASK, (b) QPSK and (c) 16QAM. As shown in the figure, the estimated SNR values are quite

TABLE 2. Recognition accuracies for different modulation types by employing all features (10-fold cross-validation).

Signal types			
Recognized / Actual	250 Mbps 2ASK	500 Mbps QPSK	1 Gbps 16QAM
250 Mbps 2ASK	**100%**	-	-
500 Mbps QPSK	0.48%	**99.51%**	-
1 Gbps 16QAM	-	-	**100%**

close to the actual ones. The mean SNR estimation errors are 0.61 dB, 1.09 dB, 0.67 dB for 2ASK, QPSK and 16QAM respectively.

Table 2 summarizes the recognition accuracies for three signal types by employing all features. The overall recognition accuracy is calculated by taking the average of the three individual accuracies on the diagonal of Table 2 (in bold font). The average value of the accuracies of the individual signal types is 99.83% despite the fact that the signals are deteriorated by both noise and multipath fading.

The relationship between the number of selected features and the identification accuracy for two different types of K-fold cross-validation (K = 5, K = 10) is depicted in Fig. 12.

It is observed from Fig. 12 that the recognition accuracy increases exponentially with the number of selected features. The figure highlights that when utilizing only three selected features, the classification accuracies approach 70%, but when utilizing five features and above, the recognition accuracies attain values higher than 96%. Also as shown in the figure, if the selected number of features is 5 or higher, the effect of increasing the chosen number of features on improving the classification accuracy is slightly noticeable. It is worth to mention that all these high accuracies have been realized with the consideration of a real-world scenario, i.e., multipath fading channel.

Fig. 13 illustrates the effect of tuning the number of selected features on the mean SNR estimation error for the testing data set using 5-fold and 10-fold cross-validation methods. It is obvious from the figure that both parameters have inversely proportional relationship. In other words, when the number of selected features increases, the mean estimation error of SNR decreases and vice versa. When the most six significant features are selected, the obtained average estimation errors using both 10 and 5-fold cross-validation methods are quite similar i.e., 1 dB and 1.02 dB, respectively. On the other hand, when using more than 6 features, the average estimation error values are consistently less than 1 dB. Moreover, it is clear from the figures 12 & 13 that there is no significant effect of testing data set's size on the overall determination accuracies. In other words, it proves that there is no biasing to any class of the three modulation types in the testing data set.

The results shown in Fig. 12 and Fig. 13 are presented numerically in Table 3 for the 10-fold cross-validation method. It is observed from the table that when

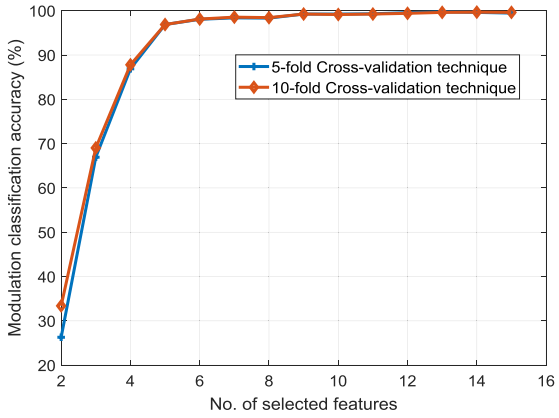

FIGURE 12. Effect of number of PCs selected on the overall identification accuracy for two types of K-fold cross-validation methods.

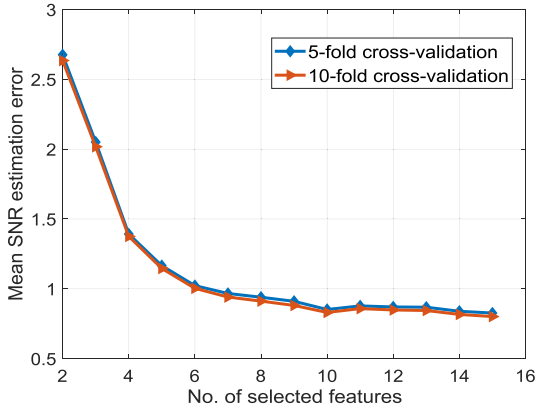

FIGURE 13. Mean estimation error of SNR as a function of the number of selected features for two types of K-fold cross-validation technique.

TABLE 3. No. of features with recognition accuracies and regression errors for the 10-fold cross-validation method.

No. of selected features	Recognition accuracy (modulation format)	Regression error (SNR)
2	33.39	2.63
3	69.03	2.01
4	87.8	1.37
5	96.88	1.14
6	98.12	1
7	98.55	0.94
8	98.44	0.91
9	99.25	0.88
10	99.14	0.83
11	99.25	0.85
12	99.41	0.84
13	99.62	0.84
14	99.68	0.81
15	99.62	0.80

the number of selected features is equal or more than 6 features, the accuracies are high and reasonably stable.

TABLE 4. Recognition accuracies for different signal types at most six significant features (10-fold cross-validation).

Modulation types (at No. of features = 6)			
Actual \ Recognized	250 Mbps 2ASK	500 Mbps QPSK	1 Gbps 16QAM
250 Mbps 2ASK	**99.34%**	0.48%	0.18%
500 Mbps QPSK	0.93%	**97.12%**	1.95%
1 Gbps 16QAM	0.14%	1.94%	**97.92%**

TABLE 5. Recognition accuracies for different signal types at most fifteen significant features (10-fold cross-validation).

Modulation types (at No. of features = 15)			
Actual \ Recognized	250 Mbps 2ASK	500 Mbps QPSK	1 Gbps 16QAM
250 Mbps 2ASK	**100%**	0	0
500 Mbps QPSK	0.66%	**99.01%**	0.33%
1 Gbps 16QAM	0	0.15%	**99.85%**

This proves the effect of exploiting the PCA technique in extracting the significant features from AAHs while reducing the complexity in terms of the required input dimensions.

Tables 4 and 5 present the confusion matrix between the identified and actual signal types at number of features 6 and 15 respectively for the 10-fold cross-validation method. The overall recognition accuracies are 98.12% and 99.62% respectively. It is clear that the increment in classification accuracies is not very significant, therefore it signifies the necessity of employing features extraction technique to gain high accuracies with less computational complexity.

The above results conclude the capability of the proposed work for joint determination of signal types and SNRs in multipath fading channels with good accuracies. Moreover, compared to the existing automatic modulation recognition (AMR) and SNR regression techniques which use coherent detection [1], [18], [19], [30]–[38], the presented work offers a simplicity in hardware implementation. This is due to the utilization of AAHs which essentially requires no timing knowledge, preceded by an envelope detection stage. Note that despite having a lower implementation complexity as compared to ADTPs-based approaches presented in [20] and [21], the proposed technique offers better estimation accuracies for signal types and SNRs. Therefore, it can be considered as an attractive alternative for low-cost multi-parameter estimation in future wireless networks. It is worth to mention that the features used in this work can be exploited using any good machine learning tool. The proposed SVM-based algorithm, which simultaneously performs both classification (using SVC) and regression (using SVR) tasks, produces very comparable results with the work in [20] which also implements two deep neural networks (DNN-1 & 2) in order to perform the two tasks.

TABLE 6. A Comparison between the DNN-based algorithm in [20] and the proposed scheme.

	Machine learning tool employed	Determination accuracies	
		Modulation recognition accuracy	Mean SNR estimation error
Ref. [20]	Two DNNs: ***DNN-1*** (modulation type), ***DNN-2*** (SNR estimation)	99.80%	1 dB
proposed technique	Two SVMs: ***SVC*** (modulation type), ***SVR*** (SNR estimation)	99.83%	0.79 dB

As shown in Table 6, the obtained results by both the DNNs and the proposed technique are almost similar in modulation recognition accuracy. In addition, the presented technique offers less error of SNR prediction i.e., 0.79 dB (in contrast to 1 dB for the DNNs-based technique). Therefore, the proposed approach gives pretty much the similar performance despite the fact of using relatively less complex machine learning tool (i.e., SVM).

It is worth pointing out that according to the work proposed in [39], authors concluded that training data associated with the proposed DNN technique should be large enough to attain accurate classification results. They also observed that SVM was faster in approaching very good accuracies than DNN i.e., sparse auto-encoder (SAE)-based technique when both learning types are trained with same size of dataset. This was imputed to the SVM's flexibility in handling dataset with small number of training samples. Hence, we considered SVM in the presented scheme to handle our dataset which was mentioned earlier.

The authors would like to affirm that beyond the considered modulations pool, the proposed algorithm can also be exploited for the determination of many other modulation types as long as their AAHs are unique and distinct from each other. For example, the pool of signal types in the proposed technique can be extended to include 8QAM, 32QAM and 64QAM signals. This is due to the uniqueness in number of their histograms peaks as illustrated in Fig. 14.

It is evident from Fig. 14 that AAHs reflect unique signatures among 8QAM, 32QAM and 64QAM signals. Also, they are still distinguishable from the signals pool considered in the proposed algorithm (shown in Fig. 3). Hence, it implies the capability of the presented work to recognize various signals (i.e., 2ASK, QPSK, 16QAM, 8QAM, 32QAM and 64QAM). On the other hand, we would like to clarify a constraint of the proposed scheme that is if the detected signal is one of M-PSK types, excluding QPSK signal, the technique is unable to recognize such types due to the resemblance in their (AAHs) to QPSK which is already considered in the modulations pool of the proposed scheme.

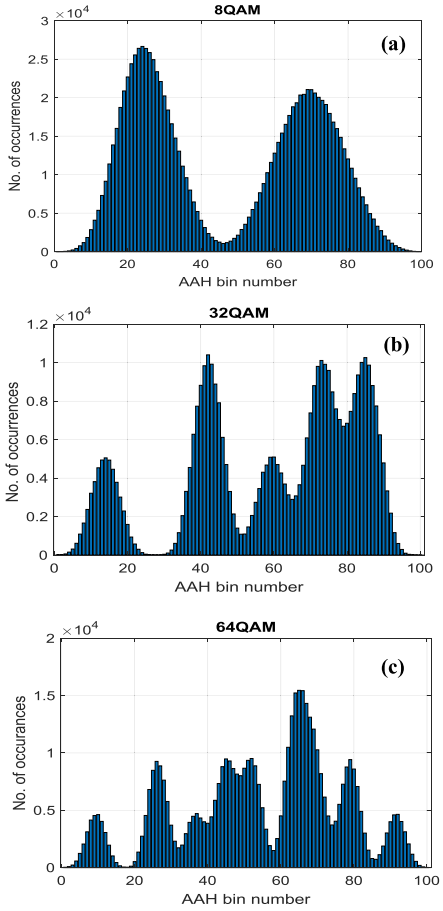

FIGURE 14. AAHs for (a) 8QAM signal, (b) 32QAM signal, (c) 64QAM signal at SNR = 22 dB.

VII. CONCLUSION

In this paper, we presented a novel technique using AAHs in combination with PCA and SVMs for joint determination of modulation types and SNRs in multipath fading channels. The proposed technique demonstrates good recognition accuracy of 99.83% for the several different modulation types. In addition, it achieves average estimation error of 0.79 dB for the SNR parameter over a large interval of 0–30 dB. The presented technique also offering much lower hardware complexity as compared to existing methods. Therefore, it is a desirable choice for simple and low-cost multi-parameter estimation in future wireless communication systems.

REFERENCES

[1] Z. Zhu and A. K. Nandi, *Automatic Modulation Classification: Principles, Algorithms and Applications*. Chichester, U.K.: Wiley, 2015.

[2] A. W. Azim, S. S. Khalid, and S. Abrar, "Non-data-aided SNR estimation method for APSK exploiting rank discrimination test," *Electron. Lett.*, vol. 48, no. 14, pp. 837–839, Jul. 2012.

[3] Y. A. Eldemerdash, O. A. Dobre, and M. Öner, "Signal identification for multiple-antenna wireless systems: Achievements and challenges," *IEEE Commun. Surveys Tuts.*, vol. 18, no. 3, pp. 1524–1551, 3rd Quart., 2016.

[4] O. A. Dobre, "Signal identification for emerging intelligent radios: Classical problems and new challenges," *IEEE Instrum. Meas. Mag.*, vol. 18, no. 2, pp. 11–18, Apr. 2015.

[5] M. D. Ming Zhang and L. Guo, "Convolutional neural networks for automatic cognitive radio waveform recognition," *IEEE Access*, vol. 5, pp. 11074–11082, 2017.

[6] A. Sengur, "Multiclass least-squares support vector machines for analog modulation classification," *Expert Syst. Appl.*, vol. 36, pp. 6681–6685, Apr. 2009.

[7] A. I. R. Fontes, A. de M. Martins, L. F. Q. Silveira, and J. C. Principe, "Performance evaluation of the correntropy coefficient in automatic modulation classification," *Expert Syst. Appl.*, vol. 42, pp. 1–8, Jan. 2015.

[8] J. J. Popoola and R. van Olst, "The performance evaluation of a spectrum sensing implementation using an automatic modulation classification detection method with a universal software radio peripheral," *Expert Syst. Appl.*, vol. 40, no. 6, pp. 2165–2173, 2013.

[9] E. Avci and D. Avci, "Using combination of support vector machines for automatic analog modulation recognition," *Expert Syst. Appl.*, vol. 36, no. 2, pp. 3956–3964, 2009.

[10] E. Avci and D. Avci, "A novel approach for digital radio signal classification: Wavelet packet energyŰmulticlass support vector machine (WPE-MSVM)," *Expert Syst. Appl.*, vol. 34, no. 3, pp. 2140–2147, 2008.

[11] A. E. Sherme, "A novel method for automatic modulation recognition," *Appl. Soft Comput.*, vol. 12, no. 1, pp. 453–461, 2012.

[12] M. L. D. Wong and A. K. Nandi, "Automatic digital modulation recognition using artificial neural network and genetic algorithm," *Signal Process.*, vol. 84, no. 2, pp. 351–365, 2004.

[13] S. Norouzi, A. Jamshidi, and A. R. Zolghadrasli, "Adaptive modulation recognition based on the evolutionary algorithms," *Appl. Soft Comput.*, vol. 43, pp. 312–319, Jun. 2016.

[14] A. Ebrahimzadeh and S. E. Mousavi, "Classification of communications signals using an advanced technique," *Appl. Soft Comput.*, vol. 11, no. 1, pp. 428–435, 2011.

[15] Z. Wu, S. Zhou, Z. Yin, B. Ma, and Z. Yang, "Robust automatic modulation classification under varying noise conditions," *IEEE Access*, vol. 5, pp. 19733–19741, Aug. 2017.

[16] M.-J. Hao, W.-L. Tsai, and Y.-C. Tsai, "Squared envelope-based SNR estimation," *J. Chin. Inst. Eng.*, vol. 36, no. 6, pp. 810–818, 2013.

[17] F. X. Socheleau, A. Aissa-El-Bey, and S. Houcke, "Non data-aided SNR estimation of OFDM signals," *IEEE Commun. Lett.*, vol. 12, no. 11, pp. 813–815, Nov. 2008.

[18] S. D. Krishnamurthy and S. L. Sabat, "Blind SNR estimation for M-ARY Frequency Shift Keying signal using covariance technique," *AEU-Int. J. Electron. Commun.*, vol. 70, no. 10, pp. 1388–1394, 2016.

[19] D. R. Pauluzzi and N. C. Beaulieu, "A comparison of SNR estimation techniques for the AWGN channel," *IEEE Trans. Commun.*, vol. 48, no. 10, pp. 1681–1691, Oct. 2000.

[20] F. N. Khan, C. Lu, and A. P. T. Lau, "Joint modulation format/bit-rate classification and signal-to-noise ratio estimation in multipath fading channels using deep machine learning," *Electron. Lett.*, vol. 52, no. 14, pp. 1272–1274, Jul. 2016.

[21] F. N. Khan *et al.*, "Automatic modulation format/bit-rate classification and signal-to-noise ratio estimation using asynchronous delay-tap sampling," *Comput. Elect. Eng.*, vol. 47, pp. 126–133, Oct. 2015.

[22] F. N. Khan, Z. Dong, C. Lu, and A. P. T. Lau, "Optical performance monitoring for fiber-optic communication networks," in *Enabling Technologies for High Spectral-efficiency Coherent Optical Communication Networks*, X. Zhou and C. Xie, Eds. Hoboken, NJ, USA: Wiley, 2016.

[23] J. Shawe-Taylor and S. Sun, "A review of optimization methodologies in support vector machines," *Neurocomputing*, vol. 74, no. 17, pp. 3609–3618, Oct. 2011.

[24] J. Han, M. Kamber, and J. Pei, *Data Mining Concepts and Techniques*, 3rd ed. Waltham, MA, USA: Morgan Kaufmann, 2012.

[25] B. Kozicki, "Chapter 12—Optical performance monitoring of optical phase-modulated signals A2—Chan, Calvin C.K," in *Optical Performance Monitoring*. Oxford, U.K.: Academic, 2010, pp. 319–350.

[26] X. Kong, C. Hu, and Z. Duan, *Principal Component Analysis Networks and Algorithms*. Singapore: Springer, 2017.

[27] I. T. Jolliffe and J. Cadima, "Principal component analysis: A review and recent developments," *Phil. Trans. R. Soc. A*, vol. 374, p. 20150202, Apr. 2016.

[28] I. T. Jolliffe, *Principal Component Analysis*, 2nd ed. New York USA: Springer-Verlag, 2002.

[29] J. E. Jackson, *A User's Guide To Principal Components*. Hoboken, NJ, USA: Wiley 2004.
[30] A. Hazza, M. Shoaib, S. A. Alshebeili, and A. Fahad, "An overview of feature-based methods for digital modulation classification," in *Proc. 1st Int. Conf. Commun., Signal Process., Appl. (ICCSPA)*, 2013, pp. 1–6.
[31] E. Soltanmohammadi and M. Naraghi-Pour, "Blind modulation classification over fading channels using expectation-maximization," *IEEE Commun. Lett.*, vol. 17, no. 9, pp. 1692–1695, Sep. 2013.
[32] M. W. Aslam, Z. Zhu, and A. K. Nandi, "Automatic modulation classification using combination of genetic programming and KNN," *IEEE Trans. Wireless Commun.*, vol. 11, no. 8, pp. 2742–2750, Aug. 2012.
[33] K. Hassan, I. Dayoub, W. Hamouda, C. N. Nzeza, and M. Berbineau, "Blind digital modulation identification for spatially-correlated MIMO systems," *IEEE Trans. Wireless Commun.*, vol. 11, no. 2, pp. 683–693, Feb. 2012.
[34] Q. Shi and Y. Karasawa, "Automatic modulation identification based on the probability density function of signal phase," *IEEE Trans. Commun.*, vol. 60, no. 4, pp. 1033–1044, Apr. 2012.
[35] A. E. Zadeh, "Automatic recognition of radio signals using a hybrid intelligent technique," *Expert Syst. Appl.*, vol. 37, no. 8, pp. 5803–5812, 2010.
[36] F. Chen, Y. Kang, H. Yu, and F. Ji, "Non-data-aided ML SNR estimation for AWGN channels with deterministic interference," *EURASIP J. Wireless Commun. Netw.*, vol. 45, pp. 1–10, 2014.
[37] Y. Li, R. Liu, and R. Wang, "A low-complexity SNR estimation algorithm based on frozen bits of polar codes," *IEEE Commun. Lett.*, vol. 20, no. 12, pp. 2354–2357, Dec. 2016.
[38] T. Salman, A. Badawy, T. M. Elfouly, T. Khattab, and A. Mohamed, "Non-data-aided SNR estimation for QPSK modulation in AWGN channel," in *Proc. IEEE 10th Int. Conf. Wireless Mobile Comput., Netw. Commun. (WiMob)*, Oct. 2014, pp. 611–616.
[39] P. Liu, K.-K. R. Choo, L. Wang, and F. Huang, "SVM or deep learning? A comparative study on remote sensing image classification," *Soft Comput.*, vol. 21, no. 23, pp. 7053–7065, 2017.

TARIK ADNAN ALMOHAMAD (S'02) received the B.Sc. degree in information engineering from the Department of Telecommunication Engineering, Ittihad Private University, Syria, in 2008, with two distinguished awards as top two performers. He was a Lab Demonstrator with Ittihad Private University from 2008 to 2010, and later he joined the wireless cooperative communication projects with Universiti Sains Malaysia (USM), Nibong Tebal, Malaysia, as a Research Assistant.

In 2012, he received the M.Sc. degree in electronic systems design engineering from USM, where he graduated as top best. He is currently pursuing the Ph.D. degree in wireless and mobile systems, where he is investigating the identification of signal's parameters in wireless communication systems. He was a recipient of USM Fellowship.

MOHD FADZLI MOHD SALLEH (M'03) was born in Bagan Serai, Malaysia. He received the B.S. degree in electrical engineering from the New York University Tandon School of Engineering, Brooklyn, NY, USA, in 1995, the M.S. degree in communication engineering from the University of Manchester Institute of Science and Technology, Manchester, U.K., in 2002, and the Ph.D. degree from the University of Strathclyde, Glasgow, U.K., in 2006. He was a Software Engineer with the Research and Development Department, Motorola, Penang, until 2001. He has supervised the eight Ph.D. degree students to graduation. He is currently an Associate Professor with the School of Electrical and Electronic Engineering, Universiti Sains Malaysia, Seri Ampangan, Nibong Tebal, Malaysia. His research interests include source coding and signal processing for application in telecommunications and wireless communication networks.

MOHD NAZRI MAHMUD received the B.Eng. degree in electronic systems engineering (telecommunications) from the Department of Electronic Systems Engineering, University of Essex, U.K., in 1996, and the M.Phil. degree in technology policy from the University of Cambridge, U.K., in 2003. He has been a Lecturer with the School of Electrical and Electronic Engineering, Universiti Sains Malaysia, since 2006. Previously, he was with Telekom Malaysia from 1996 to 2006.

ADNAN HAIDER YUSEF SA'D received the bachelor's degree in computer engineering from Hodeidah University, Yemen, 2005, and the M.Sc. degree in electronic system design engineering from Universiti Sains Malaysia, Malaysia, in 2015, where he is currently pursuing the Ph.D. degree with the School of Electrical and Electronic Engineering. He has been working in networking, wireless, and security, since 2005, and during which he owns many Cisco certificates such as CCNA, CCSP, and CCIE Security (350-018). His master's and current research interests include multicarrier transmission and PAPR reduction technique.